

A. AMBROZIAK\*, M. WINNICKI\*, P. LASKA\*, M. LACHOWICZ\*, M. ZWIERZCHOWSKI\*, J. LEŚNIEWSKI\*

## EXAMINATION OF FRICTION COEFFICIENT IN FRICTION WELDING PROCESS OF TUBULAR STEEL ELEMENTS

### BADANIE WSPÓŁCZYNNIKA TARCIA W PROCESIE ZGRZEWANIA TARCIOWEGO STALOWYCH ELEMENTÓW RUROWYCH

The paper presents a research on the relationship between friction coefficient and friction pressure (6 MPa, 12 MPa, 16.5 MPa), rotational speed (1000 rpm, 1400 rpm, 2000 rpm) and surface temperature during traditional friction welding. Values of friction pressure force and friction torque were read on an oscilloscope connected to a piezoelectric sensor and temperature was measured with a thermovision camera on circumference of the welding surface and in the heat-affected zone. Friction was measured between two tubular elements OD 18 mm x WT 2 mm. It was found that the friction coefficient is dependent mostly on pressure force and temperature. Its value ranges from 0.12 to 0.83, with the top value at 16.5 MPa and 1400 rpm.

*Keywords:* friction welding, friction coefficient, torque

Badano zależność współczynnika tarcia od wielkości docisku (6, 12 i 16,5 MPa), prędkości obrotowej (1000, 1400 i 2000  $\text{min}^{-1}$ ) oraz temperatury na powierzchni elementów podczas konwencjonalnego zgrzewania tarcioowego. Wartości siły docisku oraz momentu tarcia odczytano z oscyloskopu podłączonego do czujnika piezoelektrycznego, natomiast pomiaru temperatury dokonano kamerą termowizyjną na obwodzie powierzchni zgrzewania oraz w strefie wpływu ciepła. Badano tarcie dwóch elementów rurowych o średnicy 18 mm i grubości ścianek 2 mm. Stwierdzono, że wartość współczynnika tarcia, wykazuje największą zależność od wielkości docisku i temperatury. Współczynnik tarcia wyniósł od 0,12 do 0,83, przy czym największą wartość wykazano dla docisku 16,5 MPa i 1400  $\text{min}^{-1}$ .

### 1. Introduction

In many areas, the friction welding method more and more often replaces the traditional bonding methods. It is widely applied in industry, first of all thanks to its high performance and possibility of binding similar and dissimilar materials, both steels and non-ferrous metals and their alloys, with no necessity to use additional materials. It is important that, during the process, maximum temperature does not exceed melting points of the bonded materials.

In the presented examinations, the method of traditional friction welding was applied. The process consists in bonding two parts, one of them placed in a stationary fixture and the other rotating around their common axis, see Fig. 1. At least the rotating part should be rotationally symmetrical.

The first period of the friction welding process is named the friction period. A clamp brings the parts together until the surfaces get in touch and the friction phenomenon starts. This results in heat generation and,

as a consequence, in heating the parts to a high temperature close but not exceeding their melting point. So, the process runs in solid state and the weld is created thanks to creep of the softened material and diffusion

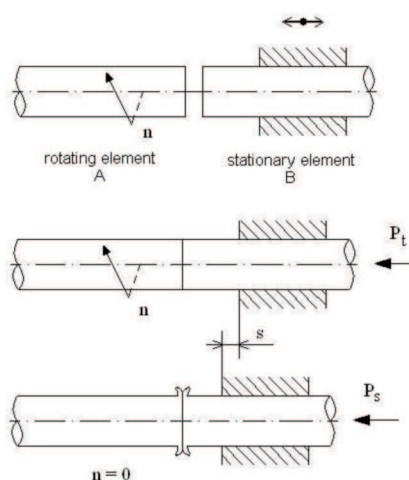


Fig. 1. Schematic presentation of friction welding:  $n$  – rotational speed;  $P_t$  – pressure force during friction period;  $P_s$  – pressure force during upsetting period;  $s$  – shortening

\* WROCLAW UNIVERSITY OF TECHNOLOGY, MECHANICAL FACULTY, 50-370 WROCLAW, 5 LUKASIEWICZA STR., POLAND

in the contact area. In the subsequent stage, called the upsetting period, increased pressure is usually applied, called the upsetting pressure [1].

Knowledge of the friction coefficient at a specific temperature for the given friction couple permits more exact calculations with the finite element method of both temperature and deformations in the joint. So far, it was accepted in the research works that the friction coefficient value is constant [2], which can lead to potential calculation errors. However, in a few works carried-out it was proved that the friction coefficient value is variable [3,4].

For the first time, a temperature-dependent friction coefficient was used during modelling by Sluzalec [5]. The author determined distributions of temperature and deformations in the friction-welding process of mild steel. In the developed model of inertia welding of two similar specimens, Moal and Massoni [6] introduced a friction coefficient changing together with rotational speed and pressure force. Zhang and others [7] presented a three-dimensional model of friction welding of nickel-based alloy specimens. However, the equation describing dependence of the friction coefficient on pressure force, temperature and rotational speed was not clearly defined, and the constants in the equation were not determined.

Vairis [3] suggests reasonably that, in order to correctly design a manufacturing process with significant role of friction, like friction welding, it is necessary to determine friction characteristics of the material used in the given conditions.

## 2. Test stand and methodology

For examinations, a multiradial drilling machine RF50 made by Csepel, Hungary, was applied, equipped with a variable-speed gear allowing 6 rotational speeds 355, 500, 710, 1000, 1400 and 2000 rpm.

Pressure force and torque were measured with piezoelectric sensors located in a measurement sleeve in that the fixture for the stationary part was installed. Schematic presentation of the test stand is shown in Fig. 2 a and its view in Figs 3 a and b. The data were read-out from a digital oscilloscope Tektronix TDS5054B. Temperature was measured with a thermovision camera made by FLIR SYSTEMS, model ThermoVision A320, that permits transferring the image in real time in the MPEG-4 format with resolution 640 x 480 pixels and frequency 30 Hz. High sensitivity of the camera (<70 mK / +30°C) ensures obtaining clear images with measurement accuracy of ± 2°C. During examinations, the camera was placed at a distance of 1 m from the test stand.

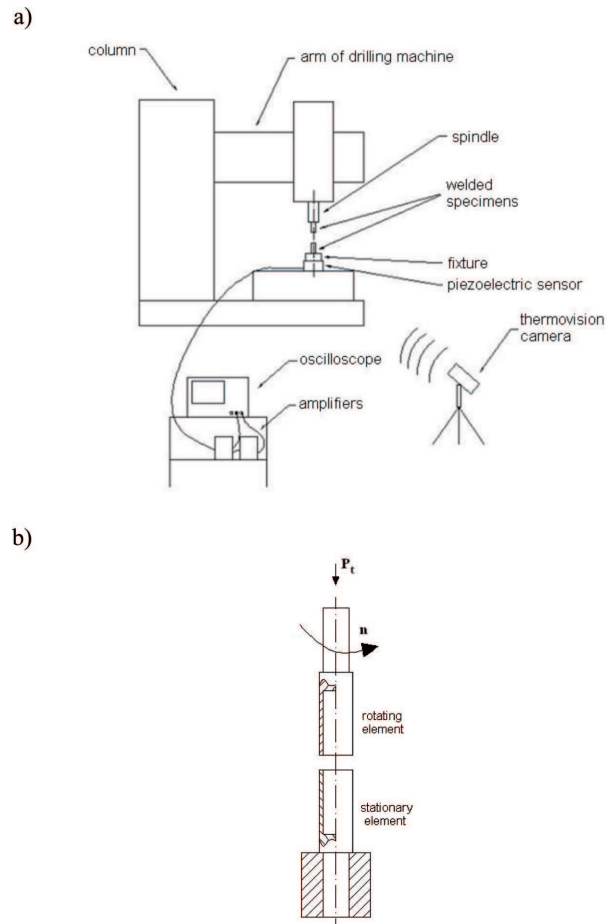


Fig. 2. Schematic presentation of the test stand (a) and fixture of the welded specimens (b)

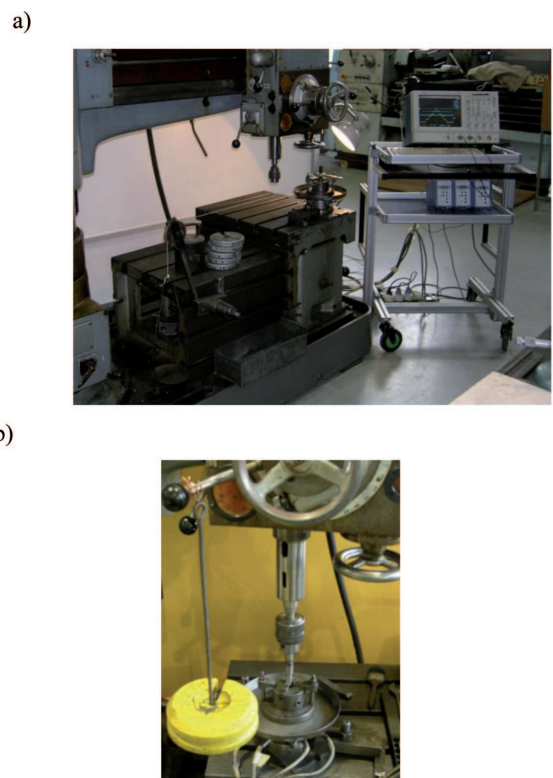


Fig. 3. View of test stand with fixed specimens: general view (a), friction welding stand (b)

An image from the thermovision camera was saved on a computer disk and next processed and analysed by means of a suitable software that lead to conclusions on the reached temperatures in relevant places on the specimens.

An exemplary read-out of the oscilloscope is shown in Fig. 4. The line marked "1" shows the torque values and that marked "2" shows the pressure force.

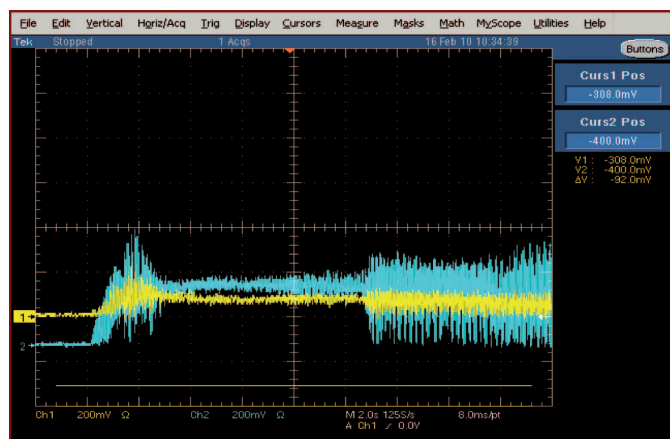


Fig. 4. View from the oscilloscope screen – an exemplary read-out

For the research reasons, some special hollow specimens were prepared, OD 18 mm x WT 2 mm, see Figs. 2 b and 5. The specimens were made of the unalloyed steel S235. The steel was in isotropic elastoplastic condition, with density  $\rho = 7850 \text{ kg/m}^3$ , linear expansion coefficient  $\alpha = 12 \times 10^{-6} \text{ K}^{-1}$  and thermal conductivity coefficient  $\lambda = 58 \text{ W/m}\cdot\text{K}$ .

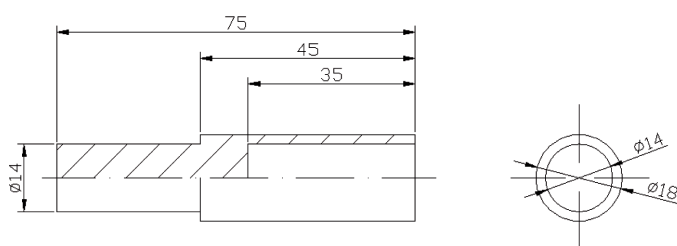


Fig. 5. Specimens used for testing

The research was aimed at determining the friction coefficient in function of temperature at various parameters of the process, close to the real friction welding process.

### 3. Experiments

#### 3.1. Temperature measurements

Figures 6 and 7 show exemplary test results recorded as diagrams of axial force, torque and temperature on the friction surface depending on variable welding parameters, i.e. rotational speed (1000 and 1400 rpm) and friction pressure (6 and 12 MPa). It was assumed that the measured torque was generated by the friction force and thus determined as "the friction torque". Its maximum value is indicated in the temperature diagrams.

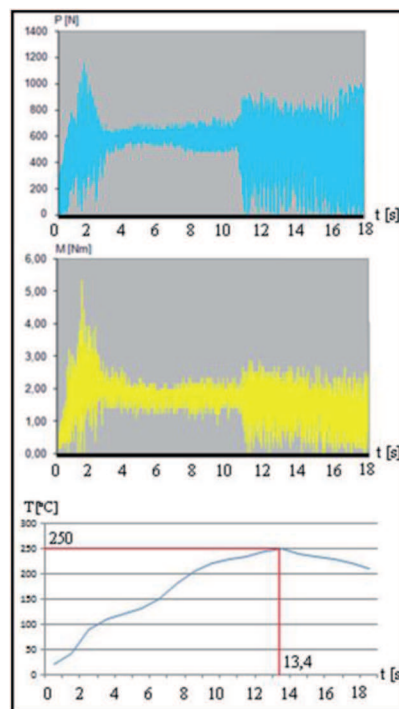


Fig. 6. Diagram of pressure force, friction torque and temperature as functions of time for  $n = 1000 \text{ rpm}$  and  $P_f = 595 \text{ N}$

TABLE 1

Parameters used in the tests

Pressure force $P_f$ , N (pressure, MPa) Rotational speed $n$ , rpm	595 N (6 MPa)	1190 N (12 MPa)	1657.5 N (16.5 MPa)
1000	Fig. 6	v	v
1400	v	Fig. 7	v
2000	v	v	v

The friction welding process was carried-out at constant pressure force, with 3 values of 6, 12 and 16.5 MPa. The parameters used for testing are settled in Table 1.

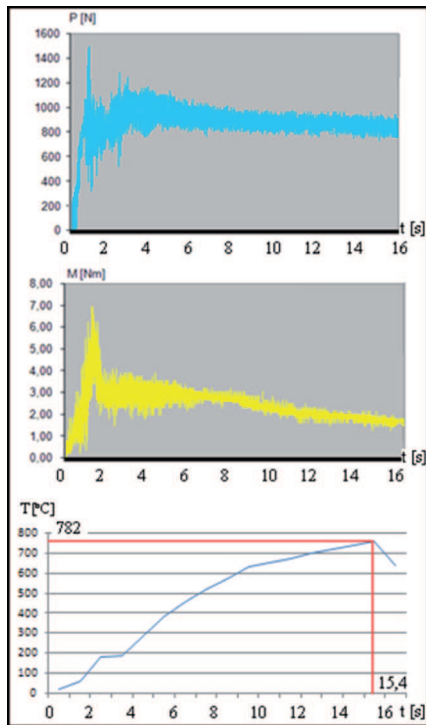


Fig. 7. Diagram of pressure force, friction torque and temperature as functions of time for  $n = 1400$  rpm and  $P_t = 1190$  N

### 3.2. Determination of friction coefficient

The obtained time-relationships of pressure force, friction torque and temperature made grounds for determining the value of friction coefficient at a given temperature.

The friction coefficient was calculated from the formula:

$$\mu = \frac{M_t}{r \cdot P_t} \tag{1}$$

where:

- $M_t$  – friction torque, Nm,
- $P_t$  – pressure force, N,
- $r$  – radius of the welded specimens ( $r = 8$  mm).

Table 2 shows the temperatures at which maximum and minimum values of friction coefficient were found for the examined parameters of the friction welding process.

Figures 8 to 10 show the calculated values of friction coefficient depending on pressure force and temperature, for fixed rotational speed.

TABLE 2

Friction coefficients calculated using various parameters of friction welding

Pressure force $P_t$ , N (pressure, MPa) Rotational speed $n$ , rpm	595 N (6 MPa)	1190 N (12 MPa)	1657.5 N (16.5 MPa)
1000	$\mu_{max} = 0.74$ $T = 40^\circ\text{C}$	$\mu_{max} = 0.73$ $T = 75^\circ\text{C}$	$\mu_{max} = 0.71$ $T = 225^\circ\text{C}$
	$\mu_{max} = 0.18$ $T = 235^\circ\text{C}$	$\mu_{max} = 0.15$ $T = 440^\circ\text{C}$	$\mu_{max} = 0.24$ $T = 804^\circ\text{C}$
1400	$\mu_{max} = 0.70$ $T = 60^\circ\text{C}$	$\mu_{max} = 0.69$ $T = 150^\circ\text{C}$	$\mu_{max} = 0.83$ $T = 90^\circ\text{C}$
	$\mu_{max} = 0.12$ $T = 470^\circ\text{C}$	$\mu_{max} = 0.19$ $T = 760^\circ\text{C}$	$\mu_{max} = 0.63$ $T = 250^\circ\text{C}$
2000	$\mu_{max} = 0.77$ $T = 85^\circ\text{C}$	$\mu_{max} = 0.67$ $T = 245^\circ\text{C}$	$\mu_{max} = 0.57$ $T = 50^\circ\text{C}$
	$\mu_{max} = 0.12$ $T = 550^\circ\text{C}$	$\mu_{max} = 0.21$ $T = 810^\circ\text{C}$	$\mu_{max} = 0.22$ $T = 730^\circ\text{C}$

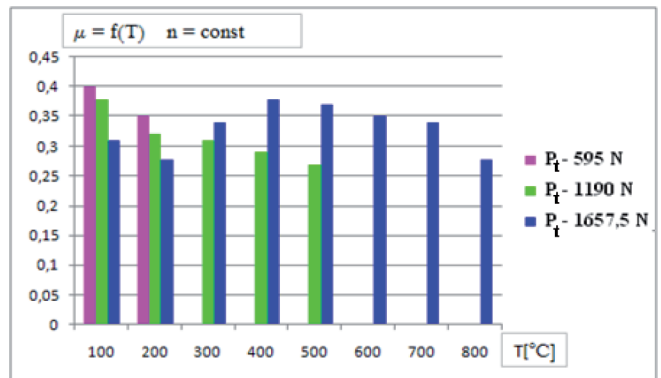


Fig. 8. Friction coefficient values depending on pressure force and temperature for  $n = 1000$  rpm

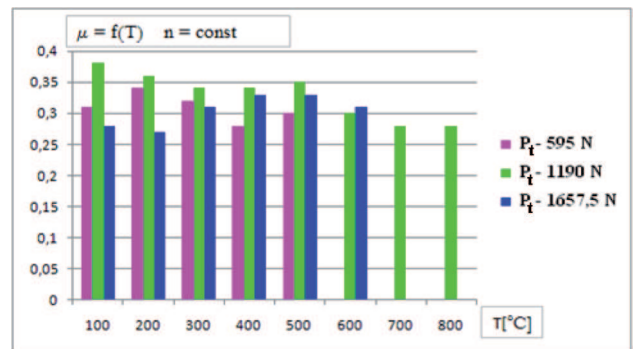


Fig. 9. Friction coefficient values depending on pressure force and temperature for  $n = 1400$  rpm

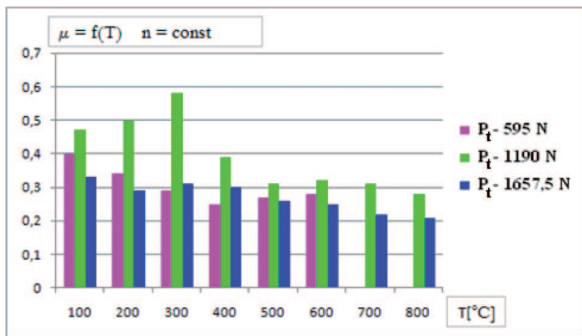


Fig. 10. Friction coefficient values depending on pressure force and temperature for  $n = 2000$  rpm

Figures 11 to 13 show the calculated values of friction coefficient depending on rotational speed and temperature, for fixed pressure force.

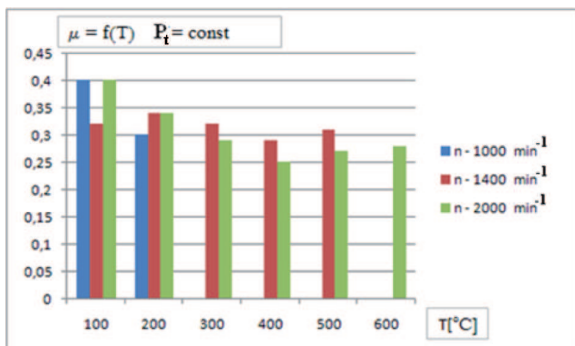


Fig. 11. Friction coefficient values depending on rotational speed and temperature for  $P_t = 595$  N

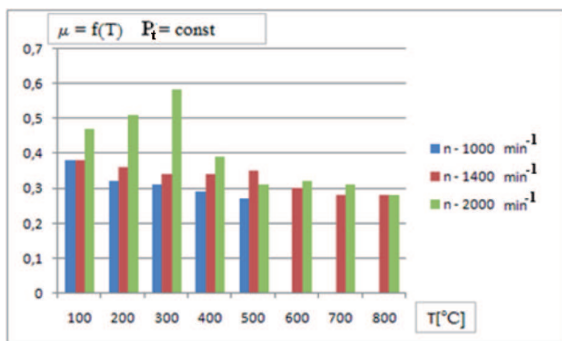


Fig. 12. Friction coefficient values depending on rotational speed and temperature for  $P_t = 1190$  N

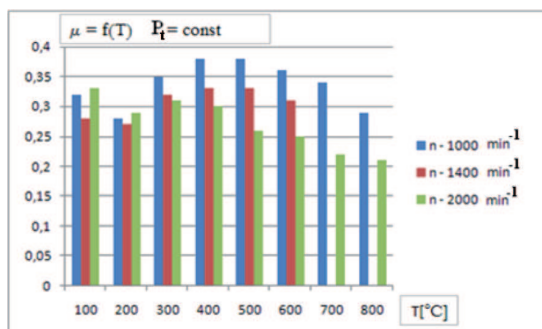


Fig. 13. Friction coefficient values depending on rotational speed and temperature for  $P_t = 1657.5$  N

#### 4. Discussion of the results

The diagrams of pressure force are characterised by nearly constant course when the friction welding process is stabilised after the initial friction period. In noticeable way it is possible to link their run with the torque diagram, because torque increases along with rising pressure force. Fluctuations of pressure force were caused by slight disturbances resulting from insufficiently stiff arm of the drilling machine and occurred especially during the initial friction period.

As for the temperature changes on the friction surface with time, temperature increases with time during welding, while the examinations were carried-out till maximum values of 600 to 800 °C. During the initial friction period, torque increases at temperatures up to ca. 250 °C and its local fluctuations are caused by tacking at the beginning of the friction process.

Variable parameters of the friction welding process, and thus rotational speed  $n$  and pressure force  $P_t$ , significantly affected the measured values. Increased rotational speed at constant pressure of 16.5 MPa resulted in reduced friction coefficient (Fig. 13), but at lower pressures and above 400 °C only slight differences were observed within the examined range of rotational speed. Increased pressure resulted in higher values of both friction torque and temperature at low rotational speed values (Fig. 8), where above 300 °C the friction coefficient changed by 0.1 between the pressure values 12 and 16.5 MPa. According to [2], increased pressure force resulted in higher deformation speed of the welded elements and in higher heating speed of the contact area.

The above-presented relationships between friction coefficient and temperature for various pressure and rotational speed values show that the friction coefficient maintains a stable value in the entire temperature range between 0.2 and 0.4 at each combination of the applied parameters. It was found that, during the initial friction period, maximum values of friction coefficient reaching over 0.7 happen at lower temperatures, see Table 2. The coefficient value declines with increasing temperature. It should be emphasised that at 800 °C the friction coefficient value did not exceed 0.3 for all the examined parameters. The highest value of 0.83 was reached at 16.5 MPa and 1400 rpm, but it was only 0.57 for 16.5 MPa and 2000 rpm. It can be assumed that the friction coefficient increases with rising pressure force, although this is not clearly visible in the diagrams showing changes of the friction coefficient at fixed rotational speed and various pressing forces [8].

## 5. Conclusions

## REFERENCES

The research consisted in friction welding of steel specimens and measuring changes of friction torque, axial pressing force and temperatures on the friction surface in time, as necessary for determining the friction coefficient.

The following conclusions can be formulated:

1. Maximum values of friction coefficient were found at the initial friction period, when temperature on the specimen surface did not exceed 250°C; they ranged from 0.57 to 0.83 depending on the process parameters.
2. After reaching a temperature over 400°C on the friction surface, the friction coefficient was stabilised at ca. 0.3, while its value declined slightly with increasing temperature.
3. Increase of pressure from 6 MPa to 12 MPa resulted in increased friction coefficient.
4. At fixed pressure of 16.5 MPa and temperatures on the friction surface above 300°C, the friction coefficient values were lower for higher rotational speeds.
5. The temperatures reached on the friction surfaces were affected by both pressure force and rotational speed. The highest temperatures were reached at the highest values of the mentioned parameters. Any increase of one of the parameters resulted in higher temperature on the friction surface of the welded elements.

- [1] J. P i l a r c z y k, Engineer's Handbook – Welding Technology **2**, WNT, Warsaw 2005 (in Polish).
- [2] A. A m b r o z i a k, Temperature distribution in friction welded joints of dissimilar refractory metals, Advances in Manufacturing Sciences and Technology, Polish Academy of Science **26** (3), 39-54 (2002).
- [3] A. V a i r i s, Investigation of frictional behaviour of various materials under sliding conditions, European Journal of Mechanics Series **6**, 929-945 (1997).
- [4] M. M a a l e k i a n, E. K o z e s c h n i k, H.P. B r a n t n e r, H. C e r j a k, Comparative analysis of heat generation in friction welding of steel bars, Acta Materialia **56**, 2843-2855 (2008).
- [5] A. S ł u ż a l e c, Thermal effects in friction welding, International Journal of Mechanical Science **32** (6), 467-478 (1990).
- [6] A. M o a l, E. M a s s o n i, Finite element modelling of the inertia welding of two similar parts, Engineering with Computers **12** (6), 479-512 (1995).
- [7] Q.Z. Z h a n g, L.W. Z h a n g, W.W. L i u, X.G. Z h a n g, W.H. Z h u, S. Q u, 3D rigid viscoplastic FE modelling of continuous drive friction welding process, Science and Technology of Welding & Joining **11**, 737-743 (2006).
- [8] A. G o n t a r z, A. D z i u b a ń s k a, Ł. O k o ń, Determination of friction coefficients at elevated temperatures for some Al, Mg and Ti alloys, Archives of Metallurgy and Materials **56**, 2, 379-384 (2011).